Biological Psychiatry: GOS

Archival Report

RBFOX1 and Working Memory: From Genome to Transcriptome Revealed Posttranscriptional Mechanism Separate From Attention-Deficit/Hyperactivity Disorder

Yuanxin Zhong, Na Zhang, Feng Zhao, Suhua Chang, Wei Chen, Qingjiu Cao, Li Sun, Yufeng Wang, Zhiyuan Gong, Lin Lu, Dong Liu, and Li Yang

ABSTRACT

BACKGROUND: Many psychiatric disorders share a working memory (WM) impairment phenotype, yet the genetic causes remain unclear. Here, we generated genetic profiles of WM deficits using attention-deficit/hyperactivity disorder samples and validated the results in zebrafish models.

METHODS: We used 2 relatively large attention-deficit/hyperactivity disorder cohorts, 799 and 776 cases, respectively. WM impairment was assessed using the Rey Complex Figure Test. First, association analyses were conducted at single-variant, gene-based, and gene-set levels. Deeper insights into the biological mechanism were gained from further functional exploration by bioinformatic analyses and zebrafish models.

RESULTS: Genomic analyses identified and replicated a locus with rs75885813 as the index single nucleotide polymorphism showing significant association with WM defects but not with attention-deficit/hyperactivity disorder. Functional feature exploration found that these single nucleotide polymorphisms may regulate the expression level of *RBFOX1* through chromatin interaction. Further pathway enrichment analysis of potential associated single nucleotide polymorphisms revealed the involvement of posttranscription regulation that affects messenger RNA stability and/or alternative splicing. Zebrafish with functionally knocked down or genome-edited *rbfox1* exhibited WM impairment but no hyperactivity. Transcriptome profiling of *rbfox1*-defective zebrafish indicated that alternative exon usages of *snap25a* might partially lead to reduced WM learning of larval zebrafish.

CONCLUSIONS: The locus with rs75885813 in *RBFOX1* was identified as associated with WM. Rbfox1 regulates synaptic and long-term potentiation–related gene *snap25a* to adjust WM at the posttranscriptional level.

https://doi.org/10.1016/j.bpsgos.2022.08.006

Working memory (WM) is the ability to maintain and manipulate information in the brain/central nervous system to guide goal-directed behaviors, requiring gene expression control. WM impairments are a common trait of many psychiatric disorders, especially attention-deficit/hyperactivity disorder (ADHD) (1). ADHD has an estimated prevalence of 5.9% in school-age children; with core symptoms of inattention, hyperactivity, and impulsivity, children with ADHD usually exhibit impairments in WM (2). WM defects are the leading cause of academic failure in patients with ADHD (3), yet the underlying genetic and neurobiological bases are still not fully understood.

To date, studies of the etiology of ADHD have identified only a few variants of candidate genes, largely due to the heterogeneous nature of clinical phenotypes (4). Endophenotypes, on the other hand, may play important roles in unveiling the psychopathological processes of most psychiatric disorders. In this sense, WM defect is a reliable and promising endophenotype that could combine various pathways, including neurotransmission systems, ion channels, transcription regulators, and neurodevelopmental genes (5–9). In the neurotransmission system, the genes of presynaptic components, such as calcineurin, *DTNBP1*, dysbindin, *GAD1*, and *SNAP25* (10–15); postsynaptic proteins, such as *AKT/AKT1*, *GRIN1*, *GRIN2B*, *NOS1*, and *NRG1* (16–20); their interacting factors, such as *DAO* and *OLFM3* (21–23); and some transcriptional regulators, such as *PAWR*, *TBX1*, *ZNF804A*, *DGCR8*, and *CYFIP1* (24,25), are all associated with WM. Such a research strategy to pick up candidate genes related to WM defects has shed light on the understanding that defects in the neurotransmission system contribute significantly to WM deficiency.

Visual WM is crucial in processing visual information. Its deficiencies are linked to general dysfunction in cognition (26) and presented as one of the important symptoms in several psychiatric disorders (27,28). Zebrafish, a kind of vertebrate, has high similarity in physiological structure, growth, and development process with human beings and has shown high conservatism in evolution, making it a hot model organism in

ISSN: 2667-1743

the field of biomedical research in recent years (29,30). Although the central nervous system of zebrafish is different from that of mammals, several key brain regions of zebrafish are homologous to that of mammals (31). The behavioral patterns of zebrafish and mammals are also quite similar. Zebrafish can show high-level behavior and neural integration, including memory, conditioned reflex, and social behavior (32,33). In this study, we performed genomic analyses of visuospatial WM in a relatively large number of children with ADHD and validated the genetic variants significantly associated with WM abnormality. We further tested the affected gene in zebrafish, taking advantage of this highly tractable model system (29,30).

METHODS AND MATERIALS

Subjects: Discovery and Replication Cohorts

Two consecutive ADHD samples were recruited from our child psychiatric clinics, which included 1040 cases in the discovery cohort and 1192 cases in the replication cohort. Both cohorts were medication free and between 6 and 16 years of age. All cases met DSM-IV ADHD diagnostic criteria based on a semistructured interview by senior child and adolescent psychiatrists using the Clinical Diagnostic Interview Scale. The other inclusion criteria were as follows: Full Scale IQ $\geq$ 70 and both biological parents were of Han descent. Those who had comorbidities with major neurological or psychiatric disorders, such as schizophrenia, bipolar disorder, major depressive disorder, pervasive development disorder, and epilepsy, were excluded. Individuals without WM measures (n = 200 and 342, respectively), age (n = 0 and 2, respectively), or IQ (n = 27 and 37, respectively) were excluded from genetic analyses (see the pipeline in Figure S11). Majority of the cases were medication naïve. If the child had been medicated, a washout period for at least 1 month was necessary before the recruitment. This work was approved by our Institutional Review board. Written informed consent was obtained from parents.

Visuospatial WM Task: Rey Complex Figure Test Delayed Component

The subject was instructed to observe a complex figure designed by Rey (34) and then was asked to draw the figure from memory onto a blank sheet of paper after 30 seconds. After a 20-minute delay, the subject was asked to recall and draw the figure from memory again. The test was scored according to the structure (0–6) and detail accuracy (0–36). The delayed structure and detail scores were the primary variables of interest in this study for their higher cognitive load. We conducted principal component analyses to extract common features from delayed structure and detail accuracy to produce an index of Rey Complex Figure Test Delayed Component (REYD), which assesses delayed WM.

Genomic and Bioinformatics Analyses of WM in Patients With ADHD

DNA Extraction and Genotyping. Genomic DNA was extracted directly from peripheral blood sample of each subject. For the first cohort, all participants were genotyped in our ADHD genome-wide association study project using Affymetrix 6.0 array (Affymetrix, Inc.). For the second cohort, Illumina Infinium PsychArray (Illumina, Inc.) was used. Both were genotyped at CapitalBio Ltd. Genotypes were called by GENOME STUDIO calling algorithm with the human reference genome (hg19). The same quality control steps were performed. Individuals with per-individual autosomal heterozygosity standard deviation larger than the mean, sex inconsistent with site reports, a per-individual call rate $<$ 95%, and the lower call rate in a pair of individuals with proportion identity by descent PI_HAT $>$ 0.185 were excluded (35). Furthermore, relatedness between the 2 cohorts was checked (PI_HAT $<$ 0.05). Then, the variants were filtered based on per–single nucleotide polymorphism (SNP) call rate $<$ 95%, deviation from Hardy-Weinberg equilibrium with $p < .001$, or a minor allele frequency $<$ 1% (35). After quality control, 1026 samples with 644,166 SNPs and 1147 samples with 284,176 SNPs remained for the 2 cohorts, respectively (pipeline shown in Figure S11). We imputed nongenotyped SNPs of the 2 cohorts using IMPUTE2, with 2186 phased haplotypes from the full 1000 Genomes Project Integrated Phase 3 Release (36) as the reference panel. We removed imputed SNPs with a squared correlation with the true genotypes $r^2 < 0.9$ or with minor allele frequency $<$ 0.01. Finally, 6,552,994 and 5,468,003 SNPs were included for the 2 cohorts, respectively, after imputation.

Genetic Single-Marker Analyses. We performed association analyses on a single SNP for REYD using PLINK version 1.9 (37). By multidimensional scaling, no substantial population stratification was found. As WM is correlated with age, sex, and IQ (38,39), we included them as covariates. Linear regression models were used with age, sex, IQ, and the top 10 eigenvectors from the genetic principal component analysis as covariates for pruned SNPs (r^2 = 0.2) by EIGENSOFT 4.2 (40). When we performed phenotypic association analyses for ADHD (i.e., ADHD diagnosis and inattention, impulsivity, and hyperactivity measures based on Clinical Diagnostic Interview Scale), all covariates mentioned above were included except IQ. Bonferroni correction was used, and $p < 5 \times 10^{-8}$ was regarded as whole-genome–wide significance. Significant loci were tested in the replication sample (corrected p [p_{CORR}] $<$ .05). Meta-analyses were also implemented in PLINK (37). All reported p values are 2-sided.

Gene-Based and Pathway Enrichment Analyses. We further conducted gene-based analyses for both REYD and ADHD using MAGMA (41). Then, we performed pathway enrichment analyses using SNPs with $p < 1 \times 10^{-4}$ from the meta-analyses as implemented in MAGMA (41) with a 35-kb upstream and 10-kb downstream window around genes as the default setting. A total of 10,185 Gene Ontology (GO) and 186 Kyoto Encyclopedia of Genes and Genomes gene sets [obtained from MSigDB (42)] were included. Competitive p values were computed and interpreted. MAGMA's built-in Bonferroni correction was used for multiple testing corrections.

Polygenic Risk Score. Then, we performed polygenic analyses to detect a shared genetic basis between WM and ADHD symptoms. Based on the association analysis on the REYD in the discovery sample, we used PRSice (43) to perform the polygenic risk score analyses to select the most precise threshold for the *p* value that predicted ADHD symptoms in both discovery and validation cohorts, respectively, with step increased *p*-value thresholds (.000001, .00001, .0001, .001, .01, .02, .03, .04, .05, .1, .2, .3, .4, .5, and 1). An empirical multiple testing correction implemented in PRSice was applied, which is based on a permutation procedure. The significance of the regression results was corrected by a permutation test with 10,000 replicates, and $\alpha = 0.001$ as suggested was used (43). We also explored whether genetic components of glutamate receptor or long-term potentiation (LTP)–related pathways were shared between WM and ADHD symptoms. We included 236 and 75 genes that belong to glutamate receptor and LTP-related pathways, respectively, according to MSigDB (42) and performed the same polygenic risk score analyses as mentioned above.

Regulatory Feature Analyses and Network Construction. We obtained the regulatory features of the significant SNPs from rSNPBase version 3.0 (44) and HaploReg version 4.1 (45), two user-friendly graphic interface web tools that integrate comprehensive information related to genomic regulation. We also searched the expression quantitative loci in the Genotype-Tissue Expression portal (46). The expression plot was generated using the Human Protein Atlas. Using STRING (47), the interacting genes network was constructed for RBFOX1 and those enriched genes from pathway analyses.

Functional Analyses of *rbfox1* in Zebrafish

Zebrafish Husbandry and Care. Zebrafish were raised at 28 °C with a density of 8 to 10 fish/L and experimented with the established standards (48). The wild-type zebrafish used in this study was Oregon AB strain/line. All zebrafish experiments were conducted according to the guidelines approved by the Institutional Animal Care and Use Committee of Southern University of Science and Technology.

Zebrafish Loss-of-Function Studies. Loss-of-function (knockdown or knockout) experiments conducted in this study were achieved by morpholino antisense oligo technique (Gene Tools Inc.), 4 guide RNAs (gRNAs)/Cas9 technique, or Cas9 ribonucleoproteins technique. To obtain mutants of zebrafish *rbfox1* to evaluate if the gene affects visuospatial memory, we used synthetic crRNA:tracrRNA (crispr RNA:transactivating crispr RNA) duplex gRNAs and Cas9 (49). Two target sequences in RNA recognition motif of Rbfox1 were chosen, and each created indels (found in each copy of the target locus of *rbfox1*) in more than 80% of injected embryos (Figure S8). Because most injected F0 embryos could be treated as true null mutants (49), we used 5 days post fertilization (dpf)–injected larval zebrafish and morpholino antisense oligo-injected morphant to conduct behavior tests. In the case of *snap25a*, 4 gRNAs (Table S4) (http://crispor.tefor.net/) were coinjected with Cas9 nuclease, and the resulting F0 fish larvae were called knockout fish or *snap25a* 4-gRNA fish.

Genotyping

Genomic DNA was extracted from 24 hours post fertilization zebrafish embryos using TIANamp Genomic DNA Kit (Tiangen). The aimed region(s) of the gene locus was amplified by gene-specific polymerase chain reaction (PCR) primers, and the expected DNA fragment was purified by QIAquick Gel Extraction Kit (Qiagen). The purified PCR product(s) was cloned for sequencing purpose (Sangon Biotech). The cloning primers sequence are listed in Table S5.

Quantitative Real-Time PCR

Total RNA was extracted from 50 wild-type or mutant larvae at 5 dpf after fixing them in TRIzol reagent (Invitrogen). A total of 1 μg RNA was reverse-transcribed to the first strand of complementary DNA with the random primer using a complementary DNA synthesis kit (Promega). Quantitative real-time PCR primers for *snap25a* and β-actin gene are listed Table S6. The quantitative reverse transcription PCR was performed in an ABI 7500 Real-Time PCR instrument (Applied Biosystems) with the SYBR green detection system, and results were normalized with β-actin expression using ΔΔCt method.

Transcriptome Sequencing Analysis

Total RNA was separately prepared from 50 larvae (5 dpf) of wild-type or *rbfox1* morphant and sequenced through the DNBSEQ platform, with the National Center for Biotechnology Information accession number GCF_000002035.6_GRCz11 as the zebrafish genome reference. The sequencing data were filtered with SOAPnuke (version 1.5.2), and then the clean reads were mapped to genome using HISAT2 (version 2.0.4). After aligning the clean reads to genes via Bowtie2 (version 2.2.5), the Beijing Genomics Institute created a database to include all annotated coding transcripts with actual number of reads/counts calculated by RSEM (version 1.2.12). Based on the hypergeometric test and corrected by Q value with a rigorous threshold ($Q \leq 0.05$), respectively, the GO and Kyoto Encyclopedia of Genes and Genomes enrichment analysis of differential gene expressions and significant levels of terms and pathways were obtained.

Zebrafish Behavioral Tests: WM

WM can be represented by habituation in zebrafish. Short-term habituation could be analyzed through repeated acoustic or visual stimulations. Free swimming 5-dpf zebrafish larvae were dispersed in a 96-well plate to sit in the observation chamber (DanioVision; Noldus). Response velocity to acoustic/vibrational or dark flash stimuli was detected and calculated by using EthoVision XT13 video-tracking software (Noldus). For the acoustic habituation assay, 10 stimuli with an acoustic intensity of 90 dB were delivered with 1-second interstimulus interval (ISI) as baseline, followed by 20 stimuli with 1-second ISI. Acoustic habituation was indicated as % acoustic habituation = [1 − (velocity of stimuli 21–30)/(response velocity of baseline)] × 100. For the visual habituation assay, a 4-block training protocol was performed without any break between blocks. Each block

consisted of 120 dark flashes with a 15-second ISI, and each dark flash lasted for 1 second. Habituation was indicated as % visual habituation = (1 – block 4/block 1) × 100 (Figure S7).

Statistical Analyses of Zebrafish Experiments

GraphPad Prism version 7.00 was used for statistical analysis of zebrafish experiments. For 2-group comparisons, one-tailed *t* test with 95% CI was used. For comparisons with 3 or more groups, one-way analysis of variance with 95% CI was used.

RESULTS

Genome-wide Association of WM and the Relationship With ADHD Symptoms at Single-Variant and Polygenic Levels

We first performed a genome-wide analysis of visuospatial WM in children with ADHD. A total of 799 and 776 cases were ultimately included in the discovery and replication stages, respectively (multidimensional scaling plots are available in the Supplement). The demographic, IQ, and cognitive phenotype data for the discovery and replication samples are presented in Table S1.

We used delayed component (REYD), which was the principal component axis score accounting for 94.1% and 91.1% variance in the discovery and validation cohorts, respectively, in the following analyses. In the discovery stage, we identified 5 significant SNPs in whole-genome–wide association analysis, among which rs75885813 was ranked on top (p_{CORR} = 3.83 × 10^{-9}). The other 4 SNPs were in high linkage disequilibrium with rs75885813 ($r^2 > 0.9$) (Table 1). Quantile-quantile plot for SNP associations is presented in Figure S2. All 5 SNPs were located on 16p13.3 (Chr16:7120001-7160000, hg19) within the *RBFOX1* gene (Figure 1). They reached statistical significance in both the replication stage ($p_{CORR} < .05$) and meta-analyses ($p_{CORR} < 5 \times 10^{-9}$). However, associations between the *RBFOX1* SNPs and core symptoms of ADHD (i.e., inattention, hyperactivity, impulsivity, and overall symptoms) were not statistically significant ($p_{CORR} > .05$, data available upon request), nor was the association for PRS weighted by WM for patients with ADHD ($p_{CORR} > .05$) (Table S2).

Associated Variants May Affect Transcriptional Regulation

Given the strong association between rs75885813 (i.e., an intron variant of *RBFOX1*) and REYD, we further examined the regulatory features of this variant, as well as its interaction networks and coexpression genes. The chromatin state analyses showed that rs75885813 is in functional regulatory regions in various tissues indicated by the enhancer-specific H3K4me1 and promoter-specific H3K4m3 markers. It also alters the regulatory motifs of some transcription factors in the brain (Table S3). The Hi-C data suggested that a chromatin loop can form between the genomic region (16:7120001-7160000, hg19) where rs75885813 is located and the promoter of *RBFOX1* (16:6040001-6080000, hg19), also suggesting a possible regulatory effect (Figure S3) on *RBFOX1* transcriptional regulation. We further constructed a network to include its interacting partners and coexpressing genes. As shown in Figure S4, the functional protein interaction analyses indicated

Table 1. Significant SNPs Identified From Genome-wide Analysis of REYD in Discovery and Replication Samples and Meta-analyses

CHR	SNP	Pos	A1	LD With rs75885813	β		SE		Coefficient *t*-Statistic		*p*		
					Discovery	Replication	Discovery	Replication	Discovery	Replication	Discovery	Replication	Meta-analysis
16	rs75885813	7,141,263	T	–	−0.669	−0.276	0.112	0.130	−5.96	−2.12	3.83×10^{-9}	0.034	3.67×10^{-9}
16	rs114891671	7,142,203	C	0.98	−0.669	−0.352	0.113	0.135	−5.90	−2.60	5.56×10^{-9}	0.0094	6.04×10^{-10}
16	rs115712598	7,142,236	T	0.98	−0.669	−0.352	0.113	0.135	−5.90	−2.60	5.56×10^{-9}	0.0094	6.04×10^{-10}
16	rs116183707	7,142,287	A	0.98	−0.669	−0.352	0.113	0.135	−5.90	−2.60	5.56×10^{-9}	0.0094	6.04×10^{-10}
16	rs7205995	7,140,331	G	0.98	−0.667	−0.35	0.113	0.135	−5.88	−2.59	6.05×10^{-9}	0.0097	6.69×10^{-10}

Five whole-genome–significant SNPs that are in high LD were identified ($r^2 > 0.8$).
CHR, chromosome; LD, linkage disequilibrium; Pos, position; REYD, Rey Complex Figure Test Delayed Component; SNP, single nucleotide polymorphism.

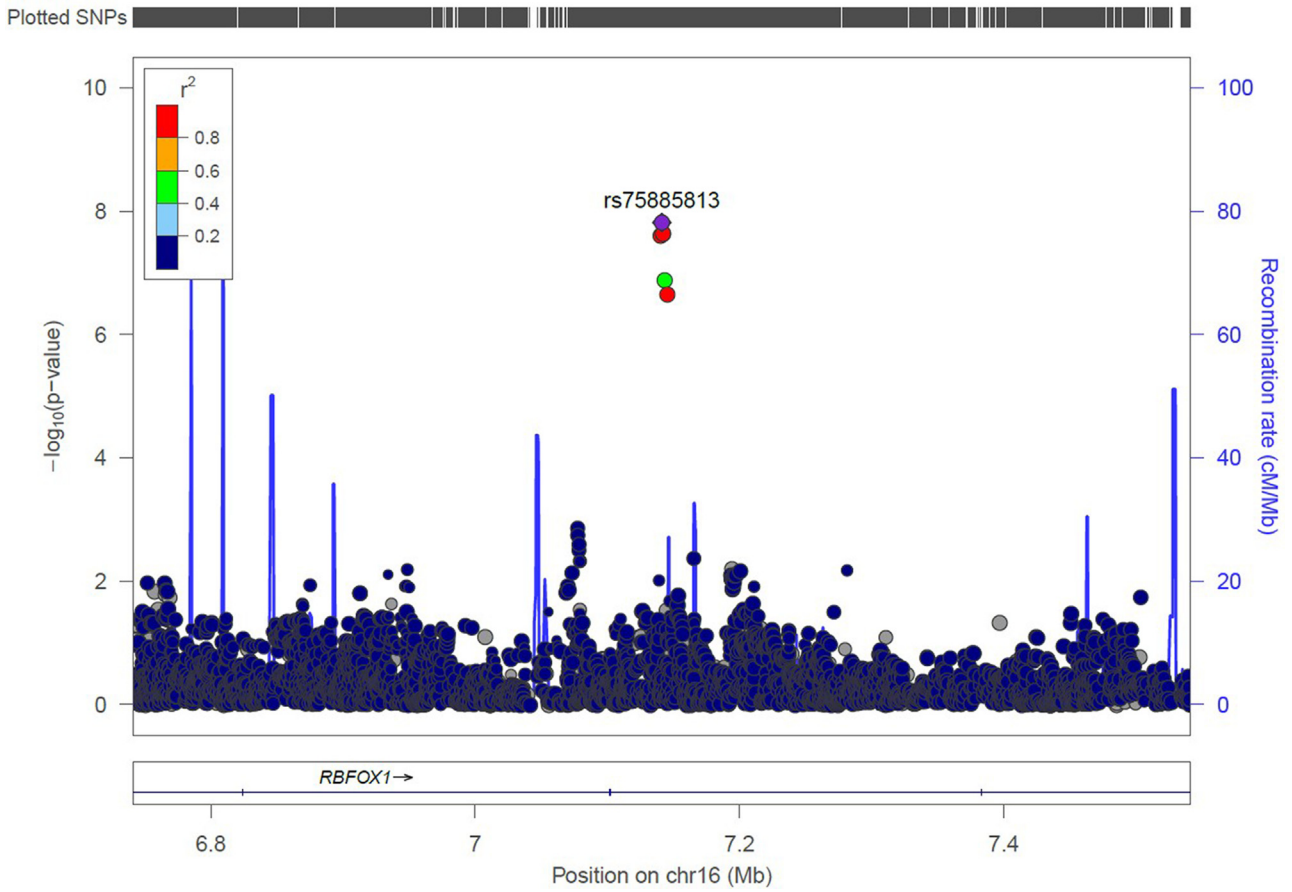

Figure 1. Regional plot of significant locus for genome-wide association of Rey Complex Figure Test Delayed Component. The gray horizontal line represents the threshold for genome-wide significant association ($p = 5 \times 10^{-8}$). rs75885813, corrected $p = 3.83 \times 10^{-9}$, was the top-ranked SNP. The other 4 significant SNPs were in high linkage disequilibrium with rs75885813 ($r^2 > 0.8$). All significant SNPs were located within *RBFOX1*. SNP, single nucleotide polymorphism.

that most of them (8 of 11) are RNA-binding proteins and may play roles in RNA alternative splicing events.

Gene-Based and Pathway Enrichment Analyses

No gene achieved significance after multiple corrections for either REYD or ADHD. We investigated subthreshold variants from the REYD association analysis using a pathway enrichment test. After removing gene sets that contained <2 genes defined in the GO analyses, 773 gene sets were included. Sixteen GO pathways reached significance ($p_{CORR} < .05$) (Figure 2 and Table 2). All of these pathways are involved in posttranscription regulation, among which the mRNA metabolic process was ranked on top. The relationships of these significantly enriched pathways are presented in Figure S5. The extended interaction gene network showed the potentially interacted genes, many of which are overlapped with risk genes for psychiatric disorders (Figure S6).

Functional Analyses of *rbfox1* in Zebrafish

To test our hypothesis that a downregulation of Rbfox1 might lead to WM defect, we first established a measurement to monitor habituation learning behaviors in zebrafish larvae. We found that during acoustic/tapping stimulation with a total of 30 taps, larval zebrafish gradually reduced the extent of their startle responses (Figure S7A, B). After exposure to a massed/continued dark flash-training period, visual habituation was also evident (Figure S7C, D). Mutant-like larval zebrafish (5 dpf), coinjected with chemically modified crRNAs/tracrRNAs and Cas9 protein against 2 sites of *rbfox1* at the 1-cell stage in wild-type fertilized eggs (Figure S8), exhibited a decrease in habituation (Figure 3A–D). The knockdown of *rbfox1* function with morpholino antisense oligos that blocked *rbfox1* pre-mRNA splicing resulted in similar habituation phenotypes (Figure 3E, F), suggesting a relationship between Rbfox1 and the WM defect in zebrafish.

Posttranscriptional Regulation of WM Genes

To select zebrafish WM-related genes in an unbiased way, we profiled the transcriptome of *rbfox1* splicing morpholino antisense oligo-injected larvae at 5 dpf. The GO and Kyoto Encyclopedia of Genes and Genomes enrichment analyses indicated that the most significantly changed pathways included the LTP, which was tightly related to memory formation, and transient receptor potential channels, which had been reported to define hippocampal synaptic transmission and WM (Figure 4A). The most affected cellular components

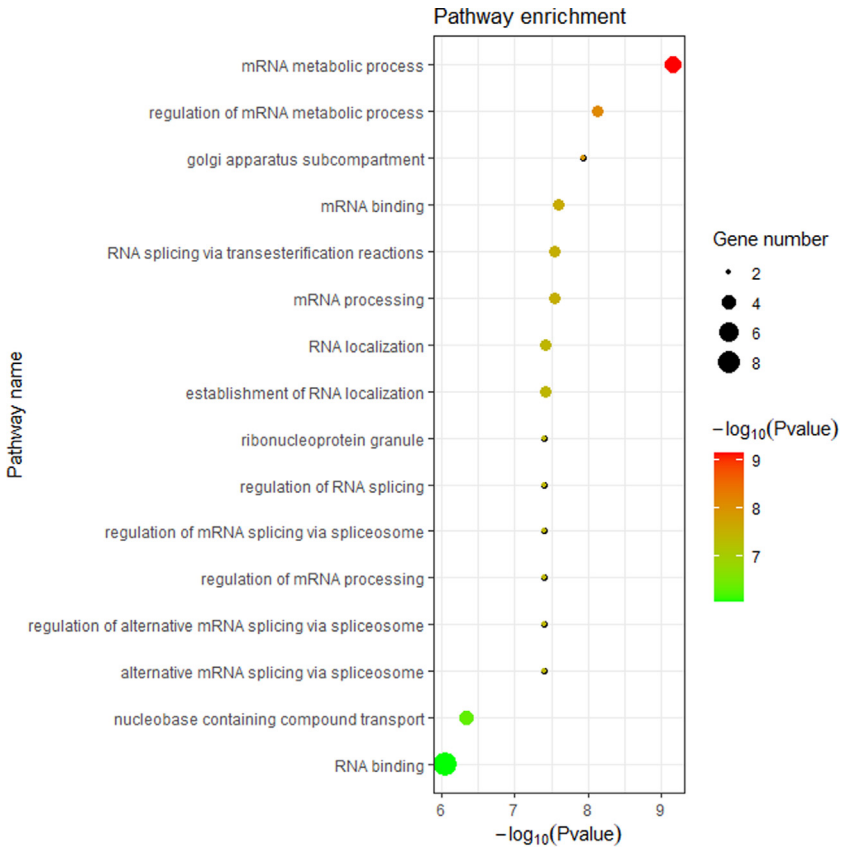

Figure 2. Bubble diagram of the pathway analysis of potentially associated variants for Rey Complex Figure Test Delayed Component. The *p* value increased from top to bottom. All the pathways displayed in the figure were significant (corrected $p < .05$). The color represents *p* value, while the size represents the number of associated genes enriched in the particular pathway. mRNA, messenger RNA.

included pre- and postsynapse connections (Figure 4B). Gene expression of proteins in postsynaptic density, the presynaptic membrane, and the ionotropic glutamate receptor complex were all significantly changed. For instance, we found that *snap25a* and *snap25b* were the most abundantly expressed genes encoding a synaptosome-associated protein in 5-dpf larvae (Figure S9).

Among well-studied neurotransmission-related genes, functional protein association analyses revealed that SNAP-25 is within a few closely related RNA processing components networked with RBFOX1 (Figure S4). Zebrafish *Snap25a* might be the most abundant synaptosome-associated protein in 5-dpf larval fish responsible for presynaptic neurotransmitter release (Figure S9A). Zebrafish *snap25a* is a homolog of mouse *Snap25*, which is known to have 2 alternative splicing variants: *Snap25a* and *Snap25b* that correspond to 2 zebrafish splicing variants, *snap25a*-202 and *snap25a*-201 transcripts (Figure S9D), respectively, during 24 to 96 hours post fertilization. Only 11 amino acids are different between Snap25a-201 and Snap25a-202, and these amino acids are all due to the alternative usage of exon-5. Apparently, *snap25a*-201 is predominantly expressed during embryogenesis and early larval stage (Figure S9C).

In *rbfox1* mutant, *snap25a*-201 transcripts were significantly decreased ($p < .01$) while *snap25a*-202 expression was significantly increased ($p < .001$) (Figure 5B). An *rbfox1* binding motif, (U)GCAUG, is found in exon 5 of *snap25a*-202, and the overall reduced *snap25a* expression level (Figure S9B) also indicates that an imbalanced expression of two splicing variants most likely changes zebrafish visuospatial memory or acoustic/vibration-mediated memory.

To obtain zebrafish *snap25a* mutants, we used another gene knockout method that produces null F0 zebrafish with high probability (50). Using a mix of 4 single-guide RNAs against *snap25a* and Cas9 to inject the yolk of fertilized eggs, we evaluated learned memory of *snap25a* mutant at 5 dpf and discovered significantly reduced acoustic/vibration and visual habituation (Figure 5A), similar to those found in *rbfox1* mutant and morphant that were responsible for the impaired short-term memory.

DISCUSSION

The past few decades have witnessed studies of many candidate genes related to the genetic vulnerability of WM impairments. However, most picked candidate genes were limited to the hypotheses. Our genome-wide single-variant and polygenic analyses of WM defects in children with ADHD identified 5 *RBFOX1* intronic variants/SNPs that may affect RBFOX1 levels in the brain. Zebrafish loss-of-function of *rbfox1* experiments showed both visual and auditory habituation defects in larval fish. When *rbfox1* was knocked down or out, *snap25a* was found downregulated and mis-spliced.

Table 2. Enriched Biological Process by Potential Associated Variants With Working Memory

Full Name	No. of Genes/Total[a]	Gene List	β	Standardized β	SE	*p*
GO:0016071 GOBP mRNA Metabolic Process	5/879	*RBFOX1*, *SMG6*, *TNFSF13*, *FXR2*, *RAVER1*	0.697	0.144	0.0995	6.963×10^{-10}
GO:1903311 GOBP Regulation of mRNA Metabolic Process	3/334	*RBFOX1*, *TNFSF13*, *FXR2*	1.511	0.244	0.235	7.520×10^{-9}
GO:0098791 GOCC Golgi Apparatus Subcompartment	2/887	*RBFOX1*, *CNGB1*	1.454	0.193	0.230	1.189×10^{-8}
GO:0003729 mRNA Binding	3/538	*RBFOX1*, *EIF4A1*, *FXR2*	1.416	0.229	0.231	2.538×10^{-6}
GO:0006397 GOBP mRNA Processing	3/543	*RBFOX1*, *FXR2*, *RAVER1*	1.350	0.218	0.222	2.917×10^{-8}
GO:0000375 GOBP RNA Splicing via Transesterification Reactions	3/384	*RBFOX1*, *FXR2*, *RAVER1*	1.350	0.218	0.222	2.917×10^{-8}
GO:0051236 GOBP Establishment of RNA Localization	3/200	*NUP205*, *RBFOX1*, *SMG6*	0.590	0.0952	0.0979	3.882×10^{-8}
GO:0006403 GOBP RNA Localization	3/233	*NUP205*, *RBFOX1*, *SMG6*	0.590	0.0952	0.0979	3.882×10^{-8}
GO:0000381 GOBP Regulation of Alternative mRNA Splicing via Spliceosome	2/57	*RBFOX1*, *FXR2*	1.370	0.181	0.228	4.009×10^{-8}
GO:0050684 GOBP Regulation of mRNA Processing	2/139	*RBFOX1*, *FXR2*	1.370	0.181	0.228	4.009×10^{-8}
GO:0048024 GOBP Regulation of mRNA Splicing via Spliceosome	2/100	*RBFOX1*, *FXR2*	1.370	0.181	0.228	4.009×10^{-8}
GO:0043484 GOBP Regulation of RNA Splicing	2/144	*RBFOX1*, *FXR2*	1.370	0.181	0.228	4.009×10^{-8}
GO:0035770 GOCC Ribonucleoprotein Granule	2/244	*RBFOX1*, *FXR2*	1.370	0.181	0.228	4.009×10^{-8}
GO:0015931 GOBP Nucleobase Containing Compound Transport	4/252	*NUP205*, *SLC28A1*, *RBFOX1*, *SMG6*	0.511	0.0948	0.0946	4.537×10^{-7}
GO:0003723 GOMF RNA Binding	9/1938	*RPN1*, *C7orf50*, *RALYL*, *RPP25L*, *RBFOX1*, *SMG6*, *EIF4A1*, *FXR2*, *RAVER1*	0.491	0.134	0.0940	8.876×10^{-7}
GO:0008380 GOBP RNA Splicing	5/478	*C2orf49*, *RBFOX1*, *USB1*, *FXR2*, *RAVER1*	1.091	0.225	0.219	2.360×10^{-6}

The pathway enrichment analyses were conducted with single nucleotide polymorphisms with $p < 1 \times 10^{-4}$ from the association analyses as implemented in MAGMA. GOBP, Gene Ontology biological processes; GOCC, Gene Ontology cellular components; GOMF, Gene Ontology molecular functions; mRNA, messenger RNA.
[a]The number of genes enriched in the pathway and the total number of genes of the pathway.

To our knowledge, this is the first study to uncover that *RBFOX1*/*rbfox1* regulates WM posttranscriptionally.

Our pathway enrichment analysis has also identified transcription regulation that is linked to WM in accordance with previous candidate gene, gene-set, and polygenic studies (24,25). Some of the regulators are important for the synthesis of proteins required during neurobiological process of WM and mRNA metabolic process. If the expression of more *RBFOX1*/*rbfox1*-regulated LTP/synaptic genes is found to be controlled at the pre-RNA splicing and mRNA stability stages, the fine and quick regulation of neural activities such as habituation, startle response, and dependent transcription could be economically and efficiently achieved.

RBFOX1/*rbfox1* is a pleiotropic gene that has been associated with 7 specific psychiatric disorders (51). The most significant SNP, rs75885813, was previously associated with Alzheimer's disease-related phenotypes in patients with Alzheimer's disease whose characteristic traits include WM deficits (52,53). The association between *RBFOX1* rs7193263 and major depression is also evident in a genome-wide association study ($p = 9.73 \times 10^{-9}$) (54). *RBFOX1* and WM were never directly associated, yet in a genome-wide gene expression study, *Rbfox1* was linked to RNA processing after memory retrieval (55). However, in this study, no association was found between hyperactivity, an ADHD core symptom, and *RBFOX1*/*rbfox1* or *snap25a*, either in the population genetic analyses or in animal experiments (Table S2 and Figure S10). We noticed that the association of *RBFOX1* was mainly driven by a major depression sample (genome-wide association study $p = 9.73 \times 10^{-9}$) among 7 psychiatric disorders (54). The *p* value for the association of ADHD was only .0065 (56). Thus, the effect of *RBFOX1* on WM is potentially not confined only to ADHD. This study further implies that *RBFOX1* may be the common susceptibility gene of psychiatric disorders via regulating WM. More association studies of *RBFOX1*-regulated neurotransmission system genes and WM may be needed to strengthen our view.

In the functional protein association networks of *RBFOX1*, SNAP25 attracted our attention. A previous study indicated that *SNAP25* is related to WM deficits in patients with ADHD (14). In our study, we found a reduction in *snap25a* and *snap25b* expression in zebrafish *rbfox1* morphant, which showed WM

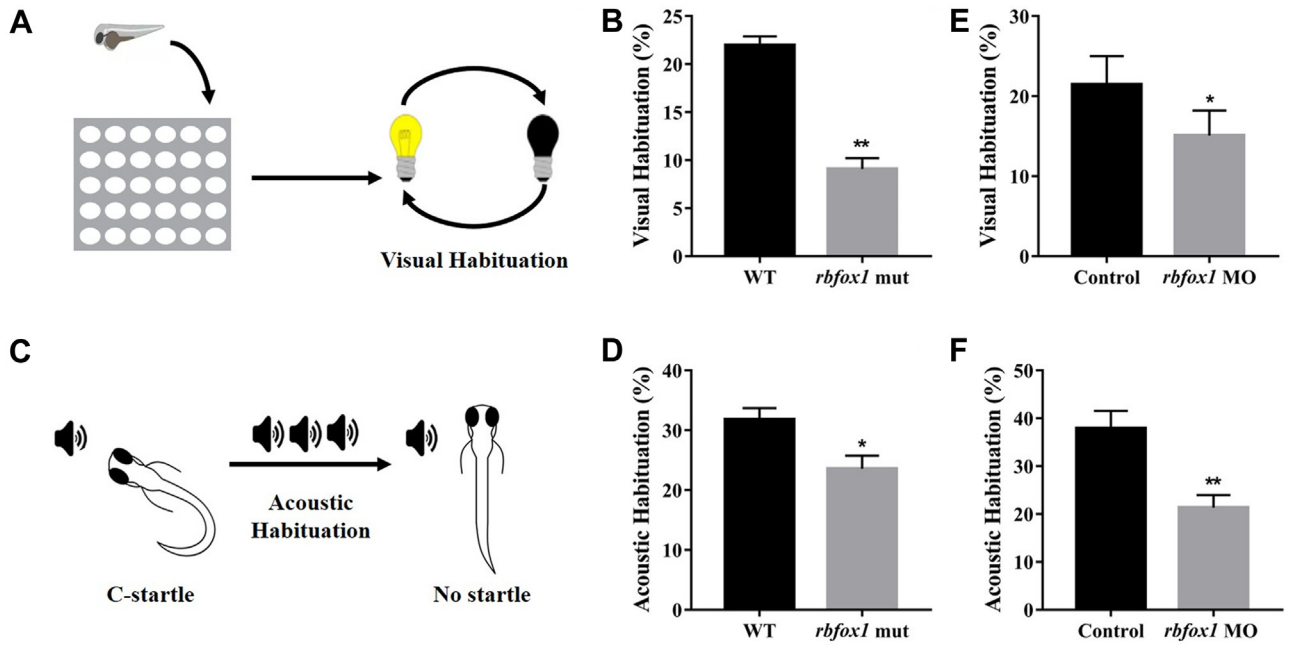

Figure 3. *rbfox1* is required for visual and acoustic habituation in larval zebrafish. **(A)** Schematic diagram of visual habituation. **(B)** Mean percentage of habituation during the visual habituation phase in the *rbfox1* mutant. **(C)** Schematic diagram of acoustic habituation. **(D)** Mean percentage of habituation during the acoustic habituation phase in the *rbfox1* mutant. **(E)** Mean percentage of habituation during the visual habituation phase in the *rbfox1* MO-injected fish. **(F)** Mean percentage of habituation during the acoustic habituation phase in the *rbfox1* MO-injected fish. The data are expressed as mean ± standard error. $n = 48$ larval fish per group. $^{*}p < .05$ (paired t test), $^{**}p < .01$. MO, morpholino antisense oligo; mut, mutant; WT, wild-type.

defect but no hyperactivity. The decrease of *snap25a* expression was more pronounced than that of *snap25b*. Zebrafish *snap25a* is homologous to mouse *Snap25*, which is known to have 2 alternative splicing variants: *Snap25a* (exon 5a, expressed late, and corresponding to zebrafish *snap25a*-202) and *Snap25b* (exon 5b, expressed early, and corresponding to zebrafish *snap25a*-201). Mouse *Snap25a* and *Snap25b* are expressed during embryonic and early postnatal development, respectively. Snap25 differentially affects interactions with other SNAREs (SNAP receptors) and SNARE-interacting proteins (57,58). The *Rbfox1*$^{-/-}$ mouse brain exhibited normal mRNA level, but decreased *Snap25b* transcripts and increased *Snap25a* transcripts (59), consistent with our findings of a decreased *snap25a-201/25a-202* ratio (Figure 5B). It is worth exploring whether reversing the *snap25a-201/25a-202* ratio or simply increasing *snap25a-201* mRNA can rescue the WM defect in *rbfox1* mutants in future studies.

However, there were some limitations in this study. First, due to the limited sample sizes, this study is underpowered to detect other WM-related variants and unveil its genetic structure more comprehensively. Enlarging the sample size and cooperation with other groups could strengthen the statistical power.

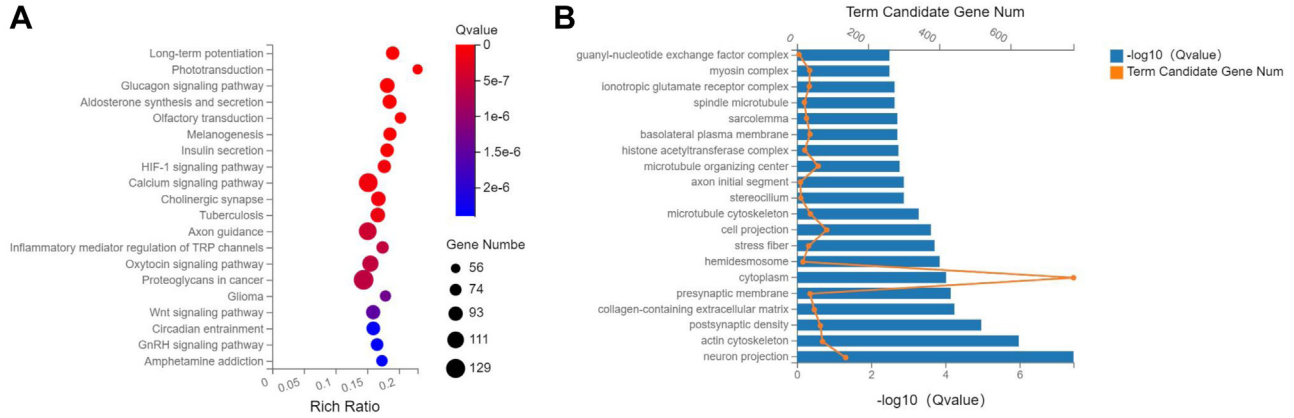

Figure 4. Zebrafish *rbfox1* regulates both presynaptic and postsynaptic functions. **(A)** Kyoto Encyclopedia of Genes and Genomes pathway enrichment of differentially expressed genes in *rbfox1* morphant. **(B)** Gene Ontology enrichment of differentially expressed genes in *rbfox1* morphant. All zebrafish larvae were collected at 5 days post fertilization, and then whole transcriptome deep sequencing was performed. HIF, hypoxia-inducible factor; GnRH, gonadotropin-releasing hormone; Num, number; TRP, transient receptor potential.

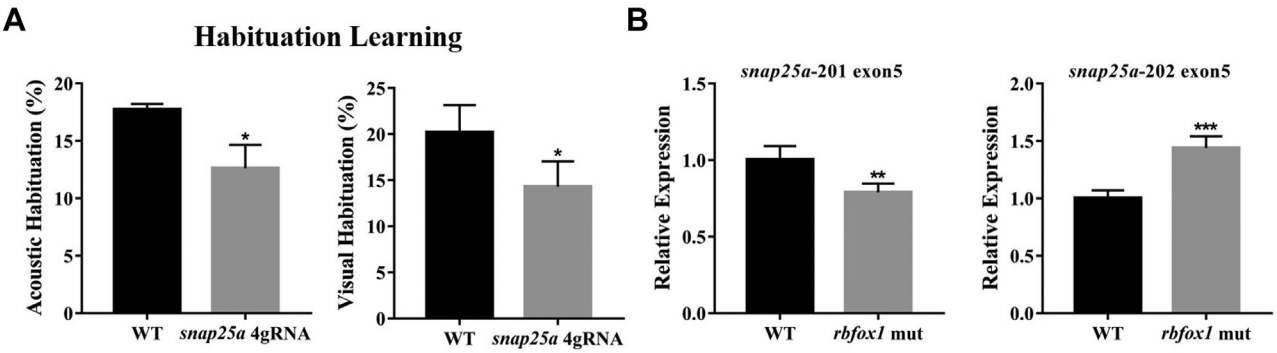

Figure 5. Posttranscriptional regulation of *snap25a* by Rbfox1. **(A)** Acoustic and visual habituation defects in *snap25a*-4sg mutant, tests performed on 5 days post fertilization, $n \geq 48$. **(B)** Changes of *snap25a* isoform ratios (exon5 alternative inclusion) in *rbfox1* mutant. The data are expressed as mean ± standard error. $n = 48$ larval fish per group. $^{***}p < .001$, $^{**}p < .01$, $^{*}p < .05$ (unpaired *t* test). 4gRNA, 4 guide RNA; mut, mutant; WT, wild-type.

In summary, these findings have revealed possible causal pathways of postranscription regulators that trigger WM deficits and alternative splicing events, mediated by Rbfox1, control SNARE, and LTP genes to affect WM.

ACKNOWLEDGMENTS AND DISCLOSURES

This work was supported by grants from National Key R&D Program of China (Grant No. 2018YFA0801006 [to DL]), National Natural Science Foundation of China (Grant Nos. 81873803 [to LY], 31771618 [to DL], and 31871259 [to SC]), the Major State Basic Research Development Program of China (973 Program, Grant No. 2014CB846100 [to YW]), National Key R&D Program of China (Grant No. 2016YFC1306103 [to QC]), National Natural Science Foundation of China (Grant Nos. 81671358 and 81761128035 [to LY]), and Shenzhen Science and Technology Innovation Committee (JCYJ20180302174233348 [to DL]).

YZ, NZ, and LY conceived the study. YZ conducted the population genetic analysis and wrote the first draft of the manuscript. NZ and FZ generated the zebrafish models, designed and conducted animal experiments, and performed the statistical analyses. WC and SC helped with the data analyses. WC and LS helped with data collection. YW helped with data collection and provided intellectual input. DL designed and directed the animal experiments. DL, LY, and LL provided intellectual input, edited the manuscript, and approved the final version.

We thank all the patients for participating in this study.

The summary statistics for the GWAS analyses will be publicly available after publication of this study. Data that support the findings of this study are available from the corresponding author upon request from qualified researchers for reasonable, noncommercial research purposes. A data application and an agreement may be required.

The authors report no biomedical financial interests or potential conflicts of interest.

ARTICLE INFORMATION

From the Peking University Sixth Hospital, Peking University Institute of Mental Health, NHC Key Laboratory of Mental Health, National Clinical Research Center for Mental Disorders, Beijing, China (YZ, SC, WC, QC, LS, YW, LL, LY); School of Life Science, Southern University of Science and Technology, Shenzhen, China (NZ, FZ, DL); Department of Biological Science, National University of Singapore, Singapore (NZ, ZG); and Peking-Tsinghua Center for Life Sciences, International Data Group, McGovern Institute for Brain Research at Peking University, Peking University, Beijing, China (LL).

YZ, NZ, and FZ contributed equally to this work.

Address correspondence to Li Yang, M.D., Ph.D., at yangli_pkuimh@bjmu.edu.cn, or Dong Liu, Ph.D., at liud@sustech.edu.cn.

Received May 27, 2022; revised Aug 9, 2022; accepted Aug 12, 2022.

Supplementary material cited in this article is available online at https://doi.org/10.1016/j.bpsgos.2022.08.006.

REFERENCES

1. Ramos AA, Hamdan AC, Machado L (2020): A meta-analysis on verbal working memory in children and adolescents with ADHD. Clin Neuropsychol 34:873–898.
2. Pievsky MA, McGrath RE (2018): The neurocognitive profile of attention-deficit/hyperactivity disorder: A review of meta-analyses. Arch Clin Neuropsychol 33:143–157.
3. Fried R, Chan J, Feinberg L, Pope A, Woodworth KY, Faraone SV, Biederman J (2016): Clinical correlates of working memory deficits in youth with and without ADHD: A controlled study. J Clin Exp Neuropsychol 38:487–496.
4. Arias-Vásquez A, Altink ME, Rommelse NN, Slaats-Willemse DI, Buschgens CJ, Fliers EA, *et al.* (2011): CDH13 is associated with working memory performance in attention deficit/hyperactivity disorder. Genes Brain Behav 10:844–851.
5. Pfeiffer P, Egorov AV, Lorenz F, Schleimer JH, Draguhn A, Schreiber S (2020): Clusters of cooperative ion channels enable a membrane-potential-based mechanism for short-term memory. eLife 9.
6. Shimshek DR, Bus T, Schupp B, Jensen V, Marx V, Layer LE, *et al.* (2017): Different forms of AMPA receptor mediated LTP and their correlation to the spatial working memory formation. Front Mol Neurosci 10:214.
7. Rashid AJ, Cole CJ, Josselyn SA (2014): Emerging roles for MEF2 transcription factors in memory. Genes Brain Behav 13:118–125.
8. Zhang CS, Bertaso F, Eulenburg V, Lerner-Natoli M, Herin GA, Bauer L, *et al.* (2008): Knock-in mice lacking the PDZ-ligand motif of mGluR7a show impaired PKC-dependent autoinhibition of glutamate release, spatial working memory deficits, and increased susceptibility to pentylenetetrazol. J Neurosci 28:8604–8614.
9. Eagle AL, Gajewski PA, Robison AJ (2016): Role of hippocampal activity-induced transcription in memory consolidation. Rev Neurosci 27:559–573.
10. Straub RE, Lipska BK, Egan MF, Goldberg TE, Callicott JH, Mayhew MB, *et al.* (2007): Allelic variation in GAD1 (GAD67) is associated with schizophrenia and influences cortical function and gene expression. Mol Psychiatry 12:854–869.
11. Kircher T, Markov V, Krug A, Eggermann T, Zerres K, Nöthen MM, *et al.* (2009): Association of the DTNBP1 genotype with cognition and personality traits in healthy subjects. Psychol Med 39:1657–1665.
12. Spangaro M, Bosia M, Zanoletti A, Bechi M, Cocchi F, Pirovano A, *et al.* (2012): Cognitive dysfunction and glutamate reuptake: Effect of EAAT2 polymorphism in schizophrenia. Neurosci Lett 522:151–155.
13. Jentsch JD, Trantham-Davidson H, Jairl C, Tinsley M, Cannon TD, Lavin A (2009): Dysbindin modulates prefrontal cortical glutamatergic

circuits and working memory function in mice. Neuropsychopharmacology 34:2601–2608.
14. Gao Q, Liu L, Chen Y, Li H, Yang L, Wang Y, Qian Q (2015): Synaptosome-related (SNARE) genes and their interactions contribute to the susceptibility and working memory of attention-deficit/hyperactivity disorder in males. Prog Neuropsychopharmacol Biol Psychiatry 57:132–139.
15. Cottrell JR, Levenson JM, Kim SH, Gibson HE, Richardson KA, Sivula M, *et al.* (2013): Working memory impairment in calcineurin knock-out mice is associated with alterations in synaptic vesicle cycling and disruption of high-frequency synaptic and network activity in prefrontal cortex. J Neurosci 33:10938–10949.
16. Pergola G, Di Carlo P, Andriola I, Gelao B, Torretta S, Attrotto MT, *et al.* (2016): Combined effect of genetic variants in the GluN2B coding gene (GRIN2B) on prefrontal function during working memory performance. Psychol Med 46:1135–1150.
17. Thomas EHX, Bozaoglu K, Rossell SL, Gurvich C (2017): The influence of the glutamatergic system on cognition in schizophrenia: A systematic review. Neurosci Biobehav Rev 77:369–387.
18. Reif A, Herterich S, Strobel A, Ehlis AC, Saur D, Jacob CP, *et al.* (2006): A neuronal nitric oxide synthase (NOS-I) haplotype associated with schizophrenia modifies prefrontal cortex function. Mol Psychiatry 11:286–300.
19. Schmitt WB, Sprengel R, Mack V, Draft RW, Seeburg PH, Deacon RM, *et al.* (2005): Restoration of spatial working memory by genetic rescue of GluR-A-deficient mice. Nat Neurosci 8:270–272.
20. Reisel D, Bannerman DM, Schmitt WB, Deacon RM, Flint J, Borchardt T, *et al.* (2002): Spatial memory dissociations in mice lacking GluR1. Nat Neurosci 5:868–873.
21. Roussos P, Giakoumaki SG, Adamaki E, Georgakopoulos A, Robakis NK, Bitsios P (2011): The association of schizophrenia risk D-amino acid oxidase polymorphisms with sensorimotor gating, working memory and personality in healthy males. Neuropsychopharmacology 36:1677–1688.
22. Heck A, Fastenrath M, Ackermann S, Auschra B, Bickel H, Coynel D, *et al.* (2014): Converging genetic and functional brain imaging evidence links neuronal excitability to working memory, psychiatric disease, and brain activity. Neuron 81:1203–1213.
23. Goldberg TE, Straub RE, Callicott JH, Hariri A, Mattay VS, Bigelow L, *et al.* (2006): The G72/G30 gene complex and cognitive abnormalities in schizophrenia. Neuropsychopharmacology 31:2022–2032.
24. Boku S, Izumi T, Abe S, Takahashi T, Nishi A, Nomaru H, *et al.* (2018): Copy number elevation of 22q11.2 genes arrests the developmental maturation of working memory capacity and adult hippocampal neurogenesis. Mol Psychiatry 23:985–992.
25. Linden DE, Lancaster TM, Wolf C, Baird A, Jackson MC, Johnston SJ, *et al.* (2013): ZNF804A genotype modulates neural activity during working memory for faces. Neuropsychobiology 67:84–92.
26. Fukuda K, Vogel E, Mayr U, Awh E (2010): Quantity, not quality: The relationship between fluid intelligence and working memory capacity. Psychon Bull Rev 17:673–679.
27. Anticevic A, Repovs G, Corlett PR, Barch DM (2011): Negative and nonemotional interference with visual working memory in schizophrenia. Biol Psychiatry 70:1159–1168.
28. Schecklmann M, Dresler T, Beck S, Jay JT, Febres R, Haeusler J, *et al.* (2011): Reduced prefrontal oxygenation during object and spatial visual working memory in unpolar and bipolar depression. Psychiatry Res 194:378–384.
29. Cassar S, Adatto I, Freeman JL, Gamse JT, Iturria I, Lawrence C, *et al.* (2020): Use of zebrafish in drug discovery toxicology. Chem Res Toxicol 33:95–118.
30. Adamson KI, Sheridan E, Grierson AJ (2018): Use of zebrafish models to investigate rare human disease. J Med Genet 55:641–649.
31. Randlett O, Wee CL, Naumann EA, Nnaemeka O, Schoppik D, Fitzgerald JE, *et al.* (2015): Whole-brain activity mapping onto a zebrafish brain atlas. Nat Methods 12:1039–1046.
32. Spence R, Gerlach G, Lawrence C, Smith C (2008): The behaviour and ecology of the zebrafish, Danio rerio. Biol Rev Camb Philos Soc 83:13–34.
33. Lieschke GJ, Currie PD (2007): Animal models of human disease: Zebrafish swim into view. Nat Rev Genet 8:353–367.
34. Shuai L, Chan RC, Wang Y (2011): Executive function profile of Chinese boys with attention-deficit hyperactivity disorder: Different subtypes and comorbidity. Arch Clin Neuropsychol 26:120–132.
35. Anderson CA, Pettersson FH, Clarke GM, Cardon LR, Morris AP, Zondervan KT (2010): Data quality control in genetic case-control association studies. Nat Protoc 5:1564–1573.
36. Sudmant PH, Rausch T, Gardner EJ, Handsaker RE, Abyzov A, Huddleston J, *et al.* (2015): An integrated map of structural variation in 2,504 human genomes. Nature 526:75–81.
37. Chang CC, Chow CC, Tellier LC, Vattikuti S, Purcell SM, Lee JJ (2015): Second-generation PLINK: Rising to the challenge of larger and richer datasets. GigaScience 4:7.
38. Valera EM, Brown A, Biederman J, Faraone SV, Makris N, Monuteaux MC, *et al.* (2010): Sex differences in the functional neuroanatomy of working memory in adults with ADHD. Am J Psychiatry 167:86–94.
39. Soares PSM, de Oliveira PD, Wehrmeister FC, Menezes AMB, Rohde LA, Gonçalves H (2022): Does IQ influence association between working memory and ADHD symptoms in young adults? 26. J Atten Disord 26:1097–1105.
40. Price AL, Patterson NJ, Plenge RM, Weinblatt ME, Shadick NA, Reich D (2006): Principal components analysis corrects for stratification in genome-wide association studies. Nat Genet 38:904–909.
41. de Leeuw CA, Mooij JM, Heskes T, Posthuma D (2015): MAGMA: Generalized gene-set analysis of GWAS data. PLoS Comp Biol 11: e1004219.
42. Liberzon A, Birger C, Thorvaldsdóttir H, Ghandi M, Mesirov JP, Tamayo P (2015): The Molecular Signatures Database (MSigDB) hallmark gene set collection. Cell Syst 1:417–425.
43. Choi SW, O'Reilly PF (2019): PRSice-2: Polygenic Risk Score software for biobank-scale data. GigaScience 8.
44. Guo L, Wang J (2018): rSNPBase 3.0: An updated database of SNP-related regulatory elements, element-gene pairs and SNP-based gene regulatory networks. Nucleic Acids Res 46:D1111–D1116.
45. Ward LD, Kellis M (2016): HaploReg v4: Systematic mining of putative causal variants, cell types, regulators and target genes for human complex traits and disease. Nucleic Acids Res 44:D877–D881.
46. GTEx Consortium (2013): The Genotype-Tissue Expression (GTEx) project. Nat Genet 45:580–585.
47. Szklarczyk D, Morris JH, Cook H, Kuhn M, Wyder S, Simonovic M, *et al.* (2017): The STRING database in 2017: Quality-controlled protein-protein association networks, made broadly accessible. Nucleic Acids Res 45:D362–D368.
48. Westerfield M (2000): The Zebrafish Book. A Guide for the Laboratory Use of Zebrafish (Danio rerio), 4th ed. Eugene: University of Oregon Press.
49. Hoshijima K, Jurynec MJ, Klatt Shaw D, Jacobi AM, Behlke MA, Grunwald DJ, *et al.* (2019): Highly efficient CRISPR-Cas9-based methods for generating deletion mutations and F0 embryos that lack gene function in zebrafish. Dev Cell 51:645–657.e4.
50. Wu RS, Lam II, Clay H, Duong DN, Deo RC, Coughlin SR (2018): A rapid method for directed gene knockout for screening in G0 zebrafish. Dev Cell 46:112–125.e4.
51. Cross-Disorder Group of the Psychiatric Genomics Consortium (2019): Genomic relationships, novel loci, and pleiotropic mechanisms across eight psychiatric disorders. Cell 179:1469–1482.e1411.
52. Stopford CL, Thompson JC, Neary D, Richardson AM, Snowden JS (2012): Working memory, attention, and executive function in Alzheimer's disease and frontotemporal dementia. Cortex J Devoted Study Nerv Syst Behav 48:429–446.
53. Herold C, Hooli BV, Mullin K, Liu T, Roehr JT, Mattheisen M, *et al.* (2016): Family-based association analyses of imputed genotypes reveal genome-wide significant association of Alzheimer's disease with OSBPL6, PTPRG, and PDCL3. Mol Psychiatry 21:1608–1612.

54. Nagel M, Jansen PR, Stringer S, Watanabe K, de Leeuw CA, Bryois J, *et al.* (2018): Meta-analysis of genome-wide association studies for neuroticism in 449,484 individuals identifies novel genetic loci and pathways. Nat Genet 50:920–927.
55. Peixoto LL, Wimmer ME, Poplawski SG, Tudor JC, Kenworthy CA, Liu S, *et al.* (2015): Memory acquisition and retrieval impact different epigenetic processes that regulate gene expression. BMC Genomics 16(suppl 5):S5.
56. Demontis D, Walters RK, Martin J, Mattheisen M, Als TD, Agerbo E, *et al.* (2019): Discovery of the first genome-wide significant risk loci for attention deficit/hyperactivity disorder. Nat Genet 51:63–75.
57. Valladolid-Acebes I, Daraio T, Brismar K, Harkany T, Ögren SO, Hökfelt TG, Bark C (2015): Replacing SNAP-25b with SNAP-25a expression results in metabolic disease. Proc Natl Acad Sci U S A 112:E4326–E4335.
58. Daraio T, Valladolid-Acebes I, Brismar K, Bark C (2018): SNAP-25a and SNAP-25b differently mediate interactions with Munc18-1 and Gβγ subunits. Neurosci Lett 674:75–80.
59. Gehman LT, Stoilov P, Maguire J, Damianov A, Lin CH, Shiue L, *et al.* (2011): The splicing regulator Rbfox1 (A2BP1) controls neuronal excitation in the mammalian brain. Nat Genet 43:706–711.